CSIRO PUBLISHING

Australian Journal of Physics

Volume 53, 2000

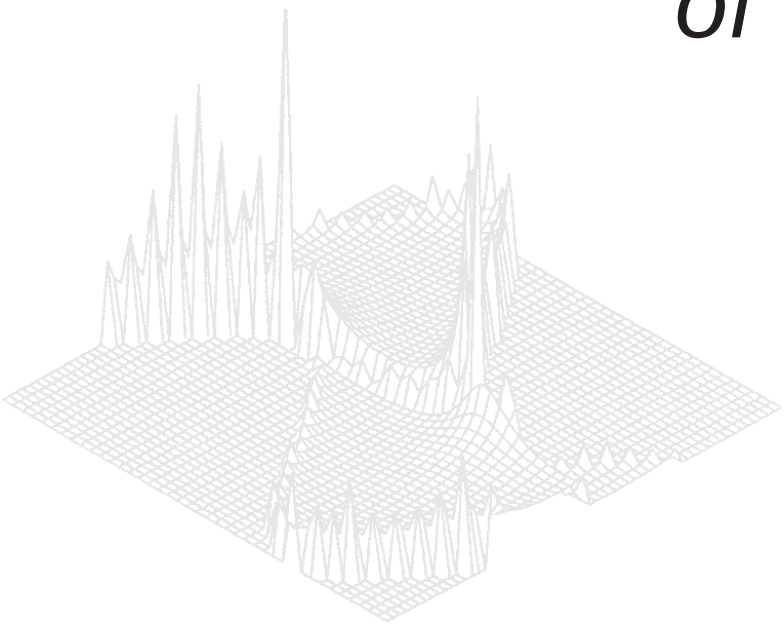

A journal for the publication of
original research in all branches of physics

www.publish.csiro.au/journals/ajp

All enquiries and manuscripts should be directed to
Australian Journal of Physics
CSIRO PUBLISHING
PO Box 1139 (150 Oxford St)
Collingwood Telephone: 61 3 9662 7626
Vic. 3066 Facsimile: 61 3 9662 7611
Australia Email: ajp@publish.csiro.au

Published by **CSIRO** PUBLISHING
for CSIRO and
the Australian Academy of Science

Aust. J. Phys., 2000, **53**, 697–705

Study of Strain Relaxation in InAs/GaAs Strained-layer Superlattices by Raman Spectroscopy and Electron Microscopy

A. K. Gutakovsky,[A] *S. M. Pintus,*[A] *A. I. Toropov,*[A] *N. T. Moshegov,*[A] *V. A. Haisler,*[A] *S. Rubanov*[B] *and P. Munroe*[B]

[A] Institute of Semiconductor Physics, Academy of Science of Russia, Siberian Branch, Novosibirsk-90, Russia.
[B] Electron Microscopy Unit, University of NSW, Sydney, NSW 2052, Australia.

Abstract

InAs/GaAs strained-layer superlattices (SLS) grown on a GaAs(100) substrate were studied by both Raman spectroscopy (RS) and transmission electron microscopy (TEM). It was shown that the interfaces inside the superlattice are coherent, but the superlattice–substrate interface contain an orthogonal two-dimensional network of 60° misfit dislocations. Using these experimental data values of elastic strain in individual layers and the average values of the residual elastic strain in SLS were determined. The latter are approximately one order of magnitude higher than theoretically predicted data, which suggests that the relaxation of elastic strains was not fully complete. Subsequent annealing of these structures led to the generation of more misfit dislocations, consistent with further relaxation of elastic strain.

1. Introduction

The degree of misfit f between individual lattices is the principal reason for the appearance of internal mechanical strains in InAs/GaAs multilayer systems. If the thickness of alternating layers in a superlattice is less than a critical value h_c, the misfit is compensated for by the elastic deformation of individual layers and the superlattice becomes a strained one. These strained-layer superlattices (SLS) represent a promising new class of optoelectronic materials. Furthermore, they are unique structures for studying the physical phenomena related to the superperiodicity of crystalline structure.

A folding of acoustic phonons branches within the limits of the Brillouin minizone deals with the effect of superperiodicity. This results in the appearance of a set of doublet peaks in the Raman scattering (RS) spectra (Colvard *et al.* 1985). Using this phenomenon the period of the superlattices can be determined by RS studies. This was done, for example, for the Ge_xSi_{1-x}/Si and InAs/GaAs superlattices (Hallivell *et al.* 1989; Shebanin *et al.* 1989). The mechanical strains in the SLS also appear in RS spectra as a displacement of the main oscillation frequency of the optical phonons. In this case, the displacement value depends on the value of mechanical strains in the layers present in the material. This effect was used for determination of the strains in strained Ge_xSi_{1-x}/Si superlattices (Hallivell *et al.* 1989).

In this work, the strained state of the InAs/GaAs superlattices grown on the GaAs substrates has been studied. The average values of the residual elastic strain in SLS has been determined, and the structure of the interfaces has been investigated by means of both RS and transmission electron microscopy (TEM).

 10.1071/PH00054 0004-9506/00/050697$05.00

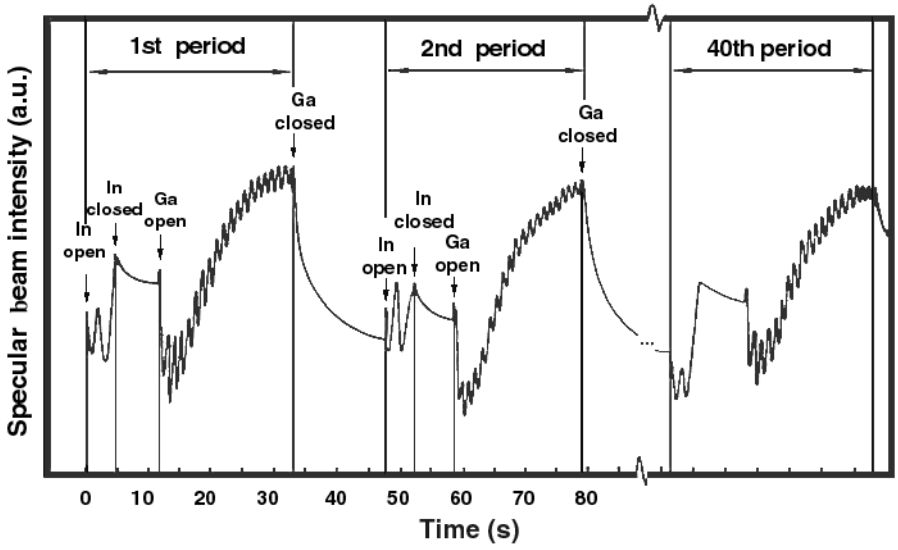

Fig. 1. Specular beam intensity during the growth of C-type SLS.

2. Experimental

(2a) The Objects of Investigation

The $[(InAs)_l(GaAs)_m]_n$ strained-layer superlattices were grown on GaAs(100) substrates by molecular beam epitaxy (MBE) in a three-chamber MBE system (Stenin 1989). The subscripts l and m denote, respectively, the number of InAs and GaAs monolayers in an individual period of the superlattice (the same subscripts are used for identification of different parameters corresponding to InAs or GaAs layers), and n denotes the number of periods of the SLS. The thickness of the InAs(100) monolayer t_l is 0.30 nm and the thickness of the GaAs(100) monolayer t_m is 0.28 nm. The methods of preparation of the substrate surface and the growth conditions were the same as described by Kanter *et al.* (1986).

The following types of SLS were grown: A-type, where $l = 2$, $m = 6$, $n = 25$; B-type, where $l = 2$; $m = 10$, $n = 40$; and C-type, where $l = 2$; $m = 19$, $n = 40$. All SLS were grown at a substrate temperature T_s of 450˚C. Growth surface monitoring was performed *in situ* using reflection high energy electron diffraction (RHEED), through the registration of the intensity of the specular electron beam. The growth rate and layer thickness in the SLS were determined according to the period of the oscillations. As shown in Fig. 1, the intensity oscillations of the specular reflected beam were observed during the whole growth process. This permitted high precision control of the thickness of individual layers and the completion of the growth of each individual layer at the moment of maximum intensity of the specular reflected beam spot that corresponded to the maximum filling of the upper monolayer (Sakamoto *et al.* 1984).

(2b) Raman Spectroscopy

The RS studies were carried out in a DFS-52 spectrometer excited by an argon laser with the wavelengths of 488 and 514.5 nm at temperatures of 10 K and 300 K in a vacuum

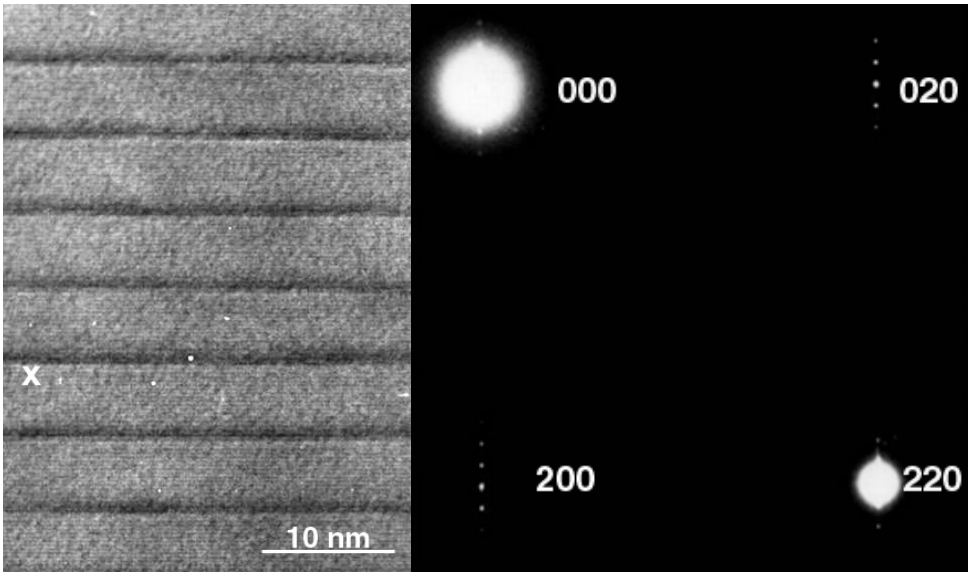

Fig. 2. HREM image of (*a*) (left) the cross section (100) of the C-type SLS and (*b*) (right) the corresponding electron microdiffraction pattern.

chamber with the Bruster geometry for quasi-back scattering. The periods of the SLS were determined by RS spectra over a range of the frequencies of acoustic phonons. The RS spectra over a range of optical phonons were used to estimate the degree of residual strain in the GaAs layers of the SLS (Colvard *et al.* 1985).

(2c) Transmission Electron Microscopy

The structure of the SLS were analysed by both conventional TEM and high resolution electron microscopy (HREM). The samples for TEM and HREM were prepared both in the form of thin foils parallel to the (001) growth surface and in the form of (100) and (110) cross sections. The plan-view (100) foils were prepared using chemical etching from the substrate side of the sample. The technique for preparation of the cross sections included mechanical thinning (Karasev 1989) with subsequent milling with argon ions. The energy of the ions was 3–5 kV and the angle of ion beam incidence was 12° (Rubanov *et al.* 1989). Electron microscope investigations were carried out with a JEOL EM-4000 EX transmission electron microscope operated at 400 kV. The periods of superlattices were determined from microdiffraction patterns. The analysis of dislocation structure was carried out under two-beam diffraction conditions using the {220}and {400} planes.

3. Results and Discussion

(3a) Structure of the SLS

A HREM image for the (100) cross section of the C-type SLS is shown in Fig. 2*a* (left). The InAs–GaAs interfaces are rather sharp (for example the region marked X). The thicknesses of the InAs layers are equal to two to three monolayers, which is in agreement with the RHEED data shown in Fig. 1. Similar results were obtained during a HREM investigation of both the A- and B-type SLS. In all cases the interfaces between individual

Table 1. Periods for A-, B- and C- type SLS measured using the RHEED, TEM and RS techniques

Type of SLS	Period of SLS in monolayers (nm)		
	RHEED	TEM	RS
A	8	6.9	8.01
B	12	11.4	11.9
C	21	19	20.9

layers are coherent and no dislocations are present. Fig. 2*b* (right) shows the electron microdiffraction pattern that corresponds to the image in Fig. 2*a*. The satellite spots caused by the diffraction of electrons by a superlattice are clearly observed near each fundamental GaAs diffraction spot. The least distance between the spots from the superlattice along the [001] direction corresponds to the value of the SLS period P which, in this instance, equals 5.32 nm. The value of P measured using the HREM image (Fig. 2*a*) and the microdiffraction pattern (Fig. 2*b*) is in broad agreement with the value of the SLS period that was determined by RHEED oscillations (Table 1), where it is assumed that

$$P = lt_l + mt_m . \tag{1}$$

Raman spectroscopy was also used to determine P. The RS spectrum for the B-type SLS is given in Fig. 3*a*. According to Shebanin *et al*. (1989), the doublet peaks arise from the scattering of the folded acoustic phonons, and their position is unambiguously associated with the period of the SLS. The values for P for all three SLS determined experimentally in this way are also listed in Table 1. It should be noted that the value of fluctuations of the SLS period that was determined from the full-width half maximum of

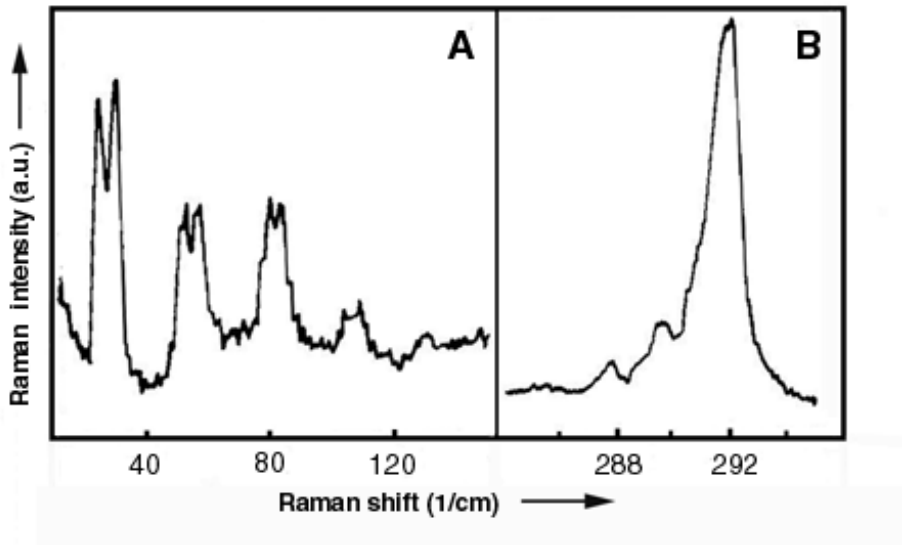

Fig. 3. Raman spectra of the B-type SLS: (*a*) scattering by folded acoustic phonons and (*b*) scattering by confined optic phonons in GaAs.

the doublet peak did not exceed one monolayer. It can be seen that the P values obtained using RS are in better agreement with the RHEED values than the TEM data. Apparently, the TEM values are more affected by local variation of growth uniformity.

The image in Fig. 2*a* was obtained from a region of the foil with a thickness of greater than 30 nm, while the objective lens defocus DF was −30 nm. The image was formed by (200), (000) and (200) electron beams. The images of the crystalline InAs and GaAs lattices are similar at such thicknesses of the foil over a wide range of defocus. The InAs layers in Fig. 2*a* were revealed only by decreasing the average level of intensity at the place of their localisation. From Fig. 2*a* one can see the interfaces in this SLS are coherent and contain no misfit dislocations (MD). In this case, the accommodation of the InAs and GaAs crystal lattices across this coherent interface is achieved through elastic strains in both layers. The elastic strains can be represented by the parameters ε_l and ε_m, which are the strains in the InAs and GaAs phases respectively. Since each crystal lattice must match at the coherent interface the signs of ε_l and ε_m must be opposite. The total misfit f is given by

$$f = |\varepsilon_l| + |\varepsilon_m| \ . \tag{2}$$

Further, the average value of the elastic strain $\bar{\varepsilon}$ for an SLS (where this symbol denotes the average value for SLS as a whole), taking into account the difference senses of the deformation of the two layers at this interface, is defined as

$$\bar{\varepsilon} = (l\varepsilon_l - m\varepsilon_m) / (l + m) \ . \tag{3}$$

However, prior to any strain relaxation of the SLS we have $\varepsilon_m = 0$ and $\varepsilon_l = f$ as shown by Lenkeit *et al*. (1989), and therefore

$$\bar{\varepsilon}_0 = fl/(l+m) = \bar{f} \ , \tag{4}$$

where $\bar{\varepsilon}_0$ is the initial elastic deformation of the SLS before relaxation, when all the misfit is accommodated by elastic strain. That is, the crystal lattice of the GaAs layers is not deformed, but the lattice of the InAs layers is tetragonally distorted. Here $\bar{f}$ is the average misfit between the SLS and the substrate.

(3b) Strain Relaxation in the SLS

By analogy with the binary systems, the process of relaxation of elastic strain in the multi-layered heterosystems becomes energetically favourable when the thickness of the SLS, H, which equals $n(t_l\, l + t_m m)$ exceeds some critical value H_c. In this case, when $H > H_c$ for each value of H, an optimal value of the average residual elastic strain $\bar{\varepsilon}_{\text{opt}}$ exists. The

Table 2. Thickness, average misfit, strain relieved, residual strain and related optimum values for the SLS obtained with the TEM and RS techniques

Type of SLS	H (nm)	$\bar{f}$ (%)	$\delta = \varepsilon_m$ (%)		$\bar{\varepsilon} = \bar{f} - \delta$ (%)		$\bar{\varepsilon}_{\text{opt}}$ (%) equation(5)
			TEM	RS	TEM	RS	
A	57	1.5	0.07	0.15	1.43	1.35	0.267
B	136	1.1	0.07	0.15	1.03	0.95	0.132
C	237	0.7	0.07	0.15	0.63	0.55	0.083

expressions for determining h_c and ε_{opt} in the binary heterosystems are usually used for mathematical definition of the values H_c and ε_{opt}. In this case the value f is substituted by $\bar{f}$ (see e.g. Matthews 1975). The values of H, $\bar{f}$ and $\bar{\varepsilon}_{opt}$ for the SLS are listed in Table 2. The value $\bar{\varepsilon}_{opt}$ was calculated from the equation

$$\overline{\varepsilon_{opt}} = b\left(1 - \nu\cos^2\varphi\right)\left(\ln H/b + 1\right) / \left[8\pi\left(1+\nu\right)\sin\varphi\cos\theta\ H\right] \quad , \tag{5}$$

where ν is the Poisson coefficient ($\nu = 0.03$), b is the Burgers vector of the MD, φ is the angle between b and the MD line, and θ is the angle between the slip plane of the MD and the plane of the interface ($\theta = 54.74^\circ$). The thicknesses of the SLS exceeded H_c values in all cases, which therefore produced the strain relaxation in all the SLS considered.

TEM studies showed that an orthogonal two-dimensional network of perfect dislocations located in the ⟨110⟩ directions is formed at the SLS–substrate interface (see Fig. 4). According to diffraction analysis, these dislocations have the same sign with $b = a/2\langle 110\rangle$ on the {111} planes. It means that they are the 60° MD ($\varphi = 60°$) formed by slip and which provide the strain relaxation in the superlattice. During such relaxation the elastic compressive deformations in the InAs layers decrease from f to ε_l and elastic tensile deformations ε_m appear in the GaAs layers. As a result, $\bar{\varepsilon}$ decreases and tends to zero with an increase in H. The value of strain relieved by formation of the MD in the SLS is defined as

$$\delta = \bar{f} - \bar{\varepsilon} \tag{6}$$

and, taking into account equations (2)–(4), is equal to ε_m. Thus, through the introduction of the MD at the SLS–substrate interface, the elastic deformation of the GaAs layers ε_m corresponds to the plastic deformation of the SLS δ.

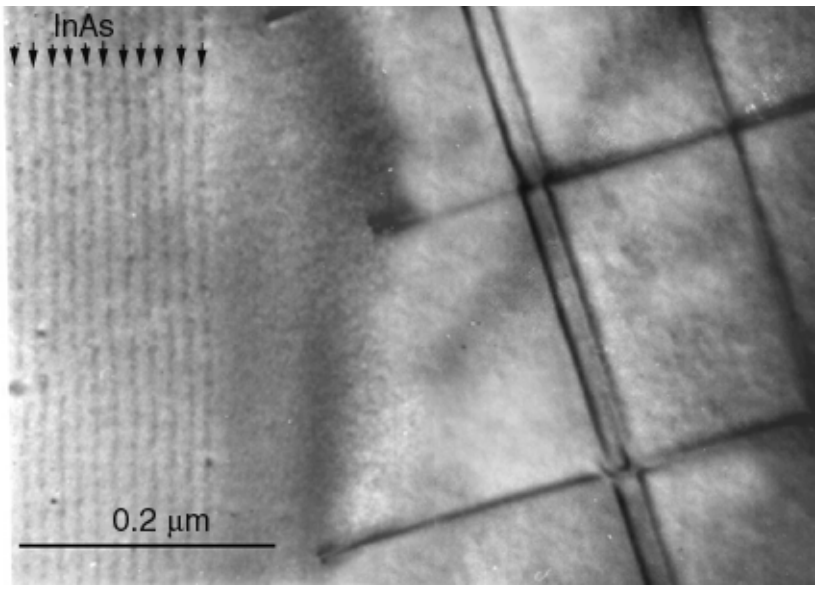

Fig. 4. Plane-view image of the C-type SLS for a wedge-shaped sample.

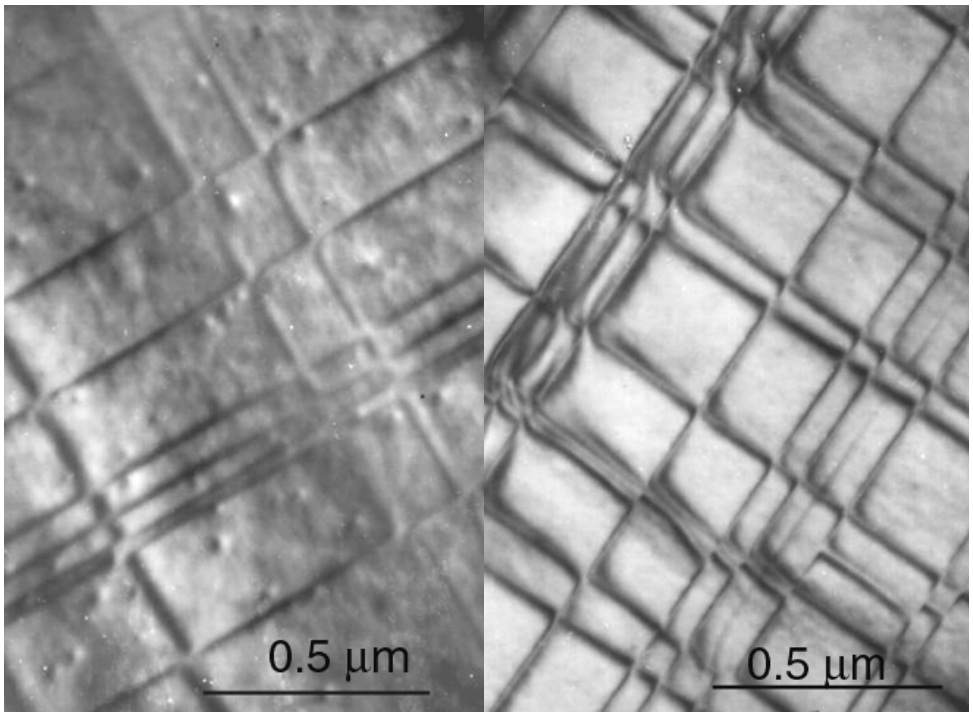

Fig. 5. TEM images of the MD in the SLS–substrate interface (*a*) (left) before and (*b*) (right) after annealing at 500°C for two hours.

Alternatively, it is known that

$$\delta = \rho\, b_e \quad , \tag{7}$$

where ρ is the linear density of the MD and b_e is the projection of the edge component b on the interface. Therefore, both the value ε_m and the value ρ can be used for quantitative description of the plastic deformation process.

The value ρ was determined from micrographs of the dislocation structure of the SLS–substrate interface. Fig. 5*a* (left) shows a typical section of the MD network of the B-type SLS. When calculating δ from equation (7) all the MD are considered as the 60° type with b_e = 0.2 nm. The accuracy of the ρ measurement was estimated to be ± 20%.

The value of elastic deformation of the GaAs layers ε_m was also estimated by Raman spectroscopy. The frequency shift of the LO phonon, Δω, relative to the frequency in a bulk, unstrained crystal (ω_{LO} = 292 cm^{-1}, Chandraschar *et al*. 1978) was measured. Account was taken of the fact that in the case of the SLS the frequency of optical phonons varies not only due to elastic deformation, but also because of the localisation effect caused by no overlap of the dispersion curves for GaAs and InAs. Hence, the GaAs LO phonons cannot penetrate the neighbouring InAs layer (Cardona 1989). This leads to the occurrence of confined optic phonons (CO phonons) with a wave vector q, which is a multiple of the value $k\pi/t_2$ (where k = 1, 2, 3 is the order of localisation). In the spectrum shown in Fig. 3*b* the last low-frequency additional peak corresponds to the CO phonon with $q \sim 7\pi/t_2$. The phonon localisation effect leads to the shift of the main peak (ω_{CO1} = 291.8 cm^{-1}) on the significantly small value of 0.2 cm^{-1} to the low frequency range. The

tensile stress also causes the shift to the low frequency range. The value of the shift is defined as

$$\Delta\omega = \varepsilon_m \left[q - P\nu / (1-\nu) \right] / \omega_{LO} \tag{8}$$

for the case of the plane strained state, where ω_{LO} is the frequency of the LO phonon in an unstrained crystal, P and q are the nonharmonic constants (Cerdeira *et al*. 1972) and ν is the Poisson coefficient. The precision of the $\Delta\omega$ measurement was estimated to be ±30%.

Experimental values of $\bar{f}$ and ε_m were used to calculate $\bar{\varepsilon}$ using equation (6). The values for ε_m, δ and $\bar{\varepsilon}$ for A-, B- and C- type SLS calculated from both TEM and RS data are listed in Table 2. In addition, values for $\bar{\varepsilon}_{opt}$ calculated from equation (5) are also shown. One can see the difference between the elastic deformation of the GaAs layers, ε_m, and the plastic deformation of the SLS, δ. However, as is shown above, these values should be equal. The differences shown in Table 2 significantly exceed the relative error of measurements for the values ρ and $\Delta\omega$ and therefore cannot be unambiguously associated with instrumental errors in either the RS or TEM measurements. The additional errors in determing ε_m can occur because a model for the plane-stressed state of the bulk elastically strained crystal (equation 8) is not suitable for the case of a plastically-strained SLS. Because of the presence of the MD the tensor for the elastic strains of each layer should differ from the plane-stressed case for such SLS. Here, the dependence of $\Delta\omega$ on the layer strain in SLS can have a more complex character in comparison with (8). This problem has not been considered in the relevant literature and is the subject of further study.

It should also be noted that the value of $\bar{\varepsilon}$ determined from (6) (taking into account the experimental values of ε_m and δ) exceeds $\bar{\varepsilon}_{opt}$ by approximately one order of magnitude. The difference observed is thought to be related to the effect of kinetic factors which limit the formation of an equilibrium MD network during SLS growth. This suggestion is confirmed by isothermal annealing of the SLS after growth. Following annealing for one hour under ultra-high vacuum at 500°C, it can be seen that the density of the MD increases by approximately a factor of 2 [see Fig. 5*b* (right)]. This means that the equilibrium level of $\bar{\varepsilon}$ and δ in the investigated heterosystem can be obtained either at the limited low growth rate or after subsequent annealing at an elevated temperature.

4. Conclusion

A combined application of TEM, HREM, RS and RHEED was used to determine a number of SLS parameters, such as the SLS periodicity, the average value of elastic strain, and the structure of the SLS–substrate interface. The thin InAs layers are visualised using HREM. The value of fluctuations of the SLS period is shown to be not greater than one monolayer of material. Raman spectroscopy allows non-destructive determination of SLS parameters. The RS measurement results are in agreement with HREM and RHEED data.

Plastic strain in the superlattices causes the formation of an orthogonal two-dimensional network of perfect dislocations at the SLS–substrate interface. These dislocations are shown to be of the same sign with the Burgers vector $b = a/2\langle 110\rangle$ in the $\{111\}$ plane (the 60° MD).

However, an analysis of the values for the residual strain $\bar{\varepsilon}$ (taking into account the experimental values ε_m and δ) shows that the relaxation of elastic strains was not complete. Apparently, this is associated with the effect of kinetic factors which limits the formation of an equilibrium MD network during the grow of SLS.

Acknowledgments

This work was supported by the Ministry of Science of Russia under the program 'Physics of Solid State Nanostructures' (grant No 3-007/2).

References

Cardona, M. (1989). *Superlattices Microstruct.* **5**, 27 .

Cerdeira, F., Buchenauer, C. J., Pollak, F., and Cardona, M. (1972). *Phys. Rev*. B **5**, 580.

Chandraschar, M., Renucei, J. B., and Cardona, M. (1978). *Phys. Rev.* B **17**, 1623.

Colvard, C., Gant, T. A., Klein, M. V., *et al.* (1985). *Phys. Rev.* B **31**, 2080.

Hallivell, M. A. G., Lyons, M. H., Davey, S. T., Hockly, M., Tuppen, C. G., and Gibbings, C. J. (1989). *Semicond. Sci. Technol.* **4**, 10.

Kanter, Yu. O, Toropov, A. I., Rzhanov, A. V., Stenin, S. I, and Gavrilova, T. A. (1986). *Poverkhnost* **9**, 83.

Karasev, V. Yu. (1989). *Zavodskaja laboratorija* **55**, 40.

Lenkeit, K., Gutakovsky, A. K., Kanter, Yu. O., *et al.* (1989). *Phys. Stat. Sol.* A **115**, 413.

Matthews, J. W. (1975). *J. Vacuum Sci. Technol*. **12**, 123.

Rubanov, S. V., Pintus, C. M., and Gutakovsky, A. K. (1989). *Pribori i Technika Experimenta* **3**, 190.

Sakamoto, T., Funabashi H., Ohta, K., Nakagawa, T., Kawai, N. T., and Kojima, T. (1984). *Jpn J. Appl. Phys*. **23**, L657.

Shebanin, A. P., Gaisler, V. A., Kurochkina, T. V., Moshegov, N. T., Stenin, S. I., and Toropov, A. I. (1989). *Pisma JETF* **49**, 349.

Stenin, S. I. (1989). *Vacuum* **36**, 419.

Manuscript received 21 June, accepted 1 August 2000